IJRRS
International Journal of Reliability, Risk Saftey: Theory and Application

Online ISSN: 2676-3346

Vol. 5/ Issue 2/ 2022/ pp. 63-77
DOI: 10.30699/IJRRS.5.2.7
Received: 2023.01.01, Accepted: 2023.02.21

Original Research Article

Direct Quantile Function Estimation Using Information Principles and Its Applications in Reliability Analysis

Jian Deng[1*]

1. Department of Civil Engineering, Lakehead University, Thunder Bay, ON, P7B5E1 Canada

*** jdeng2@lakeheadu.ca**

Abstract

Jaynes's information principle, i.e., maximum entropy principle (MEP), constrained by probability weighted moments (PWM), has been well established as an alternative method to directly estimate quantile functions (QF) from samples of a random variable. The existence, unbiasedness, and efficiency of the maximum entropy QFs have been illustrated in the literature. However, the issue of how many orders of PWMs is optimal for a given sample of data remains unsolved, and applications of the maximum entropy QFs to reliability analysis in civil engineering are still obscure. This paper serves four main purposes: (1) a new general formulation is developed for the PWM-based MEP without sample normalization; (2) the optimal order of PWMs in MEP is determined by another information principle, i.e., Akaike information criterion; (3) The feasibility of the proposed maximum entropy QFs is illustrated by two case studies in probabilistic modeling of the soil undrained shear strength and the flood frequency; (4) applications of the proposed maximum entropy QFs are substantiated in QF-based first order reliability analysis of a cantilever steel beam with uncorrelated random variables and with correlated random variables. The maximum entropy QFs are compared to common empirical probability distributions, such as normal and lognormal distributions, in reliability analysis to demonstrate the advantages and disadvantages of the method developed.

Keywords: Quantile function; Maximum entropy principle; Probability weighted moments; Akaike information criterion; Reliability analysis; Correlated random variables.

1. Introduction

Reliability and risk in engineering analysis, design, and planning have received worldwide acknowledgment [1]. Engineering parameters are commonly described by continuous random variables, and the randomness is represented by probability distributions such as probability density functions (PDF) and cumulative distribution functions (CDF). Sometimes, however, we need to know the value of the random variable corresponding to a given probability of occurrence of values smaller than the value, and this value is defined as quantile or fractile [2]. Probabilistic structural design was based on weighted fractiles [3]. A semi-probabilistic design method was also proposed by employing fractiles of distributions as a measure of structural reliability [4]. It was found that quantile-based optimization under uncertainties using adaptive kriging surrogate models can increase accuracy and efficiency [5]. A quantile-based sequential method using Kriging surrogate models was recently presented for reliability-based design optimization [6]. Another quantile-based reliability design method was proposed by Li et al. [7] and studied by He et al. [8]. A quantile-based approach was used for calibrating reliability-based partial factors [9]. A comprehensive monograph on statistical modeling with quantile functions (QF) was prepared by Gilchrist [10].

Quantile values can be calculated from QFs, which are inverse CDFs. Such quantiles often characterize the design values of loads and material properties specified by design codes [2,11]. It is often necessary to determine the quantiles of a random variable (for example, the strength of new or unknown material) from a sample of data [11,12].

If a random variable has been characterized by a known probability distribution (PDF or CDF), then the quantile is simply the point value at which the distribution function attains the specified probability. However, direct estimation of quantiles from a sample of a random variable without having a PDF or CDF is a more challenging task [11-13]. Several methods are available for the estimate of the population quantile: the prediction method, the coverage method, and the Bayesian method.

The first two are mainly empirical in that both methods need sample mean, standard deviation, and/or skewness. The Bayes method requires previous experience with a random variable. Methods were formulated to determine fractile values from statistical data, which includes information about data size [14]. Schöbi and Sudret [15] proposed a PC-Kriging-based meta-modeling method to estimate quantiles. Adaptive kriging and importance sampling were recently used in an efficient estimation of extreme quantiles [16].

In most cases, quantile estimation involves empirically choosing a common probability distribution, such as normal or lognormal distribution, and then distribution parameters are evaluated by a statistical method, such as the method of moments or method of maximum likelihood. An alternative and attractive approach for the distribution fitting comes from Jaynes' information principle, i.e., the maximum entropy principle (MEP), which provides an objective distribution-free probability distribution from observed data in terms of sample moments [17-19]. Probability-weighted moments (PWMs) [20,21] are linear combinations of the observed sample values. By interpreting PWMs as moments of quantile function, Pandey [11] derived an analytical form of quantile function using the MEP. The existence, unbiasedness, and efficiency of the maximum entropy quantile functions from samples have been well established as an alternative method to estimate quantile functions (QF) from samples of a random variable [11,22]. Entropy has been extensively applied in hydrologic and hydraulic science and engineering [23,24], but little research has touched the PWM-based entropy [17,25,26]. Furthermore, the issue of how many orders of PWMs is optimal for a given sample of data remains unsolved, which prevents this promising technique from being widely used in civil engineering. More recently, we developed maximum entropy quantile functions from a sample of data based on fractional probability weighted moments and found applications in First Order Reliability Method, a widely used method in civil engineering [27].

This paper directly estimates quantile functions using two information principles and studies their applications in reliability analysis. Section 2 introduces PWMs and interprets PWMs as the moments of quantile functions. A more general formulation without sample normalization is developed in Section 3 for PWM-based Jaynes information principle, i.e., the MEP, which is different from our previous algorithms [25-27]; Section 3 also determines the optimal order of PWMs in MEP by another information principle, i.e., Akaike information criterion (AIC); Section 4 gives illustrative case studies for the maximum entropy QF modeling in civil engineering; Section 5 substantiates the developed maximum entropy QFs in first-order reliability analysis. Conclusions are given in Section 6.

2. Probability Weighted Moments

2.1 Definition

For a random variable X, the weighted probability moment is defined by [20]

$$M_{r,s,t} = \mathrm{E}[X^r F^s (1-F)^t] = \int_0^1 [x(F)]^r F^s (1-F)^t \mathrm{d}F, F \equiv F(x) = P(X \le x), \quad (1)$$

where $M_{r,s,t}$ is the integral PWM with integral order r, s, and t. $\mathrm{E}[\cdot]$ is the mathematical expectation, F is the probability of non-exceedance. Two types of PWM are particularly interesting due to their linear combination of the random variable, Type 1:

$$\alpha_t = M_{1,0,t} = \int_0^1 x(F)(1-F)^t \mathrm{d}F = \int_0^1 x(q) q^t \mathrm{d}q \quad (2)$$

and Type 2:

$$\beta_s = M_{1,s,0} = \int_0^1 x(F) F^s \mathrm{d}F, \quad (3)$$

where $q = 1 - F$. α_t and β_s can be estimated from a sample of data by a_t and b_s, respectively,

$$\alpha_t \approx a_t = \frac{1}{n}\sum_{i=1}^n [(1-F_i)^s x_i], \quad \beta_s \approx b_s = \frac{1}{n}\sum_{i=1}^n [(F_i)^s x_i], F_i = \frac{i-0.44}{n+0.12}, \quad (4)$$

where n is the sample size, x_i is the i-th sample element, F_i is a suitable plotting position formula (e.g., the Gringorten formula) [27,40]. For an ordered sample of data, $x_1 \le x_2 \le \cdots \le x_n$, Type 1 and Type 2 integral order PWMs can be unbiasedly estimated by [21,28], respectively,

$$a_t = \frac{1}{n}\sum_{i=1}^n \left[\binom{n-i}{t} x_i\right] \Big/ \binom{n-1}{t}, \quad b_s = \frac{1}{n}\sum_{i=1}^n \left[\binom{i-1}{s} x_i\right] \Big/ \binom{n-1}{s}, \binom{n}{r} = \frac{n!}{r!(n-r)!}, \quad (5)$$

where $s, t = 0, 1, \cdots, (n-1)$ are non-negative integers.

2.2 Moments of the quantile function

Type 2 probability-weighted moment can be written as

$$\beta_s = M_{1,s,0} = \int_0^1 x(F) F^s \mathrm{d}F = \beta_0 \int_0^1 F^s \mathrm{d}T, \quad (6)$$

And

$$\mathrm{d}T = \frac{x(F)\mathrm{d}F}{\int_0^1 x(F)\mathrm{d}F}, \ \beta_0 = \int_0^1 x(F)\mathrm{d}F, \quad (7)$$

where QF, $x(F)$, is a monotonic and continuous function.

On the other hand, the ordinary raw moment (or moment about the origin) can be given by

$$E[X^s] = \int_R x^s f(x)\mathrm{d}x = \int_0^1 [x(u)]^s \mathrm{d}u, \quad (8)$$

And

$$\mathrm{d}u = \mathrm{d}F(x) = \frac{f(x)\mathrm{d}x}{\int_R f(x)\mathrm{d}x}, \ \int_R f(x)\mathrm{d}x = 1. \quad (9)$$

A similar functional form can be found between Eqs. (6) and (8), thus β_s/β_0 can be interpreted as the s-th moment of the quantile function, $x(F), 0 \le F \le 1$.

3. Information Principles

Two information principles are presented: (1) the maximum entropy principle constrained by PWMs; (2) the Akaike information criterion. The first principle is

used to generate a hierarchy of maximum entropy quantile functions from a sample of data, and the second principle will decide the optimal order of the maximum entropy quantile functions.

3.1 Maximum entropy principle

The entropy of a random variable X can be defined in terms of QF by [27]

$$H[x(F)] = -\int_0^1 [x(F)\ln x(F)]\mathrm{d}F, \quad (10)$$

where $H[x(F)]$ is the entropy, $x(F)$ is the quantile function, and F is the probability of non-exceedance. The $x(F)$ is a non-negative function for every F in the interval $[0,1]$ and is normalized to unity such that

$$\int_0^1 x(F)\mathrm{d}F = 1, \text{ (Normalization condition)} \quad (11)$$

which indicates that $\beta_0 \approx b_0 = 1$. The $x(F)$ is also satisfied constraints

$$\int_0^1 x(F)F^s\mathrm{d}F = \beta_s, s = 1,2,\cdots,K, \quad (12)$$

where K is the highest order of PWM and β_s is the s-th PWM. The β_s is estimated by b_s in Eq. (5) from a sample of data ($\beta_s \approx b_s$).

The maximum entropy principle (MEP) was created and rationalized by Jaynes [29], which states that "the minimally prejudiced assignment of probabilities is that which maximizes the entropy subject to the given information." To maximize the entropy in Eq. (10) under the constraints in Eqs. (11) and (12), the method of Lagrange multipliers is used, and the Lagrangian function $\bar{H}$ can be given by

$$\bar{H} = -\int_0^1 [x(F)\ln x(F)]\mathrm{d}F - (\eta_0 - 1)\left[\int_0^1 x(F)\mathrm{d}F - 1\right] - \sum_{s=1}^K \eta_s\left[\int_0^1 x(F)F^s\mathrm{d}F - b_s\right], \quad (13)$$

where $\bar{H}$ is the Lagrangian and η_s are the Lagrangian multipliers. $(\eta_0 - 1)$ is used as the coefficient instead of η_0 for ease of calculation. The maximization of $\bar{H}$ demands

$$\frac{\partial \bar{H}}{\partial x(F)} = 0. \quad (14)$$

Substitution of Eq. (13) into Eq. (14) yields

$$x(F) \approx x_K(F) = \exp[-\sum_{s=0}^K \eta_s F^s], \quad (15)$$

where η_s are Lagrangian multipliers and also the unknown parameters of the maximum entropy QF.

Substitution of Eq. (15) into $\ln[x(F)]$ of Eq. (10) and consideration of Eq. (12) yield a sample estimate of $H[x(F)]$,

$$\hat{H}[x(F)] = \sum_{s=0}^K (\eta_s b_s). \quad (16)$$

The Lagrangian multipliers are determined by a set of $K+1$ nonlinear equations with the sample mean $b_0 = 1$,

$$\int_0^1 F^s \exp\left[-\sum_{i=0}^K \eta_i F^i\right]\mathrm{d}F = b_s, s = 0,1,\cdots,K. \quad (17)$$

This can be done through the robust nonlinear system solver "*fsolve*" in Matlab (the Gauss-Newton method with numerical gradient and Jacobian).

If a sample mean is not unit from random variable χ, then one can normalize the sample by the sample mean to satisfy Eq. (11):

$$x = \chi/\mu. \quad (18)$$

After obtaining Eq. (15), the maximum entropy QF is given by

$$\chi_K(F) = \mu\exp\left[-\sum_{s=0}^K \eta_s F^s\right] = \exp\left[-\sum_{s=0}^K \lambda_s F^s\right], \quad (19)$$

Where

$$\lambda_0 = -\ln\mu + \eta_0, \quad (20)$$

and

$$\lambda_s = \eta_s \text{ for } s = 1,2,\cdots,K. \quad (21)$$

The normalization condition is mainly designed for interpreting PWMs as moments of quantile function in Section 2.2. It also serves to remove the effect of dimension and prevent overflow and underflow in the calculation.

If the Type-1 PWMs, α_k, are chosen as constraints of the entropy, the QF would be given as a function of the exceedance probability,

$$\chi_K(F) = \exp\left[-\sum_{i=0}^K \lambda_i(1-F)^i\right], \quad (22)$$

where $1-F$ is the probability of exceedance.

Eq. (19) or (22) is the maximum entropy QF that is estimated from a sample of data.

3.2 A general formulation of MEP without normalization

A more general algorithm of MEP is presented, where the normalization condition is relaxed. The moment constraints in Eqs. (11) and (12) can be combined as

$$\int_0^1 x(F)F^s\mathrm{d}F = \beta_s, s = 0,1,2,\cdots,K, \quad (23)$$

where β_s is the s-th PWM, and K is the highest order of PWM. If only a sample of data is available, β_s is estimated from b_s in Eq. (5), i.e., $\beta_s \approx b_s$. To maximize the entropy $H[x(F)]$ in Eq. (10), under the constraints in Eq. (23), the Lagrangian function $\bar{H}$ is given by

$$\bar{H} = -\int_0^1 [x(F)\ln x(F)]\mathrm{d}F - \sum_{s=0}^K \lambda_s\left[\int_0^1 x(F)F^s\mathrm{d}F - b_s\right], \quad (24)$$

where λ_s are unknown Lagrangian multipliers. The maximization of $\bar{H}$ requires

$$\frac{\partial \bar{H}}{\partial x(F)} = 0. \quad (25)$$

Substitution of Eq. (24) into Eq. (25) yields

$$x(F) \approx x_K(F) = \exp[-1 - \sum_{s=0}^K \lambda_s F^s]. \quad (26)$$

Substitution of Eq. (26) into $\ln[x(F)]$ of Eq. (10) and consideration of Eq. (23) yield an estimate of $H[x(F)]$ from a sample of data,

$$\hat{H}[x(F)] = b_0 + \sum_{s=0}^K (\lambda_s b_s). \quad (27)$$

The Lagrangian multipliers are determined by solving a set of nonlinear equations

$$\int_0^1 F^s \exp\left[-1 - \sum_{i=0}^K \lambda_i F^i\right]\mathrm{d}F = b_s, s = 0,1,\cdots,K. \quad (28)$$

Similar to Eq. (17), this can be done through the robust nonlinear system solver "*fsolve*" in Matlab. Similar to Eq. (22), if the Type-1 PWMs are selected as constraints of the entropy, the QF is given by,

$$x_K(F) = \exp\left[-1 - \sum_{i=0}^K \lambda_i(1-F)^i\right], \quad (29)$$

where $1-F$ is the probability of exceedance. Eq. (26) or (29) is the generalized maximum entropy QF that is derived from a sample of data without normalization.

3.3 Akaike information criterion

Sections 3.1 and 3.2 derived a maximum entropy QF from a sample of data if several PWMs were given. This section will develop a method to determine the optimal order of the maximum entropy QF from a specific sample of data. The method is based on the Akaike information criterion (AIC), which is actually a means for model selection [30].

Assume that $x(F)$ is the true but unknown QF for random variable X, $x_K(F)$ be the estimated QF based on K order PWM which is given in Eq. (19). The closeness between $x(F)$ and $x_K(F)$ can be determined by Kullback-Leibler (KL) entropy,

$$\mathrm{KL}[x(F), x_K(F)] = \int_0^1 x(F) \ln \frac{x(F)}{x_K(F)} \mathrm{d}F = C - L(\lambda, K), \tag{30}$$

where

$$C = \int_0^1 x(F) \ln x(F) \, \mathrm{d}F, \tag{31}$$

$$L(\lambda, K) = \int_0^1 x(F) \ln x_K(F) \, \mathrm{d}F. \tag{32}$$

The KL entropy is a measure of the distance between the true QF and the estimated QF, such that the smaller $\mathrm{KL}[x(F), x_K(F)]$, the closer of $x_K(F)$ to $x(F)$, and the higher quality of the fitted model $x_K(F)$. The extreme case is $\mathrm{KL}[x(F), x_K(F)] = 0$ if $x_K(F) = x(F)$. Consequently, the selection of parameters in $x_K(F)$ should minimize the KL entropy,

$$\min_k \{ \min_{\lambda_0, \cdots, \lambda_K} \{\mathrm{KL}[x(F), x_K(F)]\}\}. \tag{33}$$

The term C in Eq. (31) does not depend on $x_K(F)$, so when the KL entropy is minimized with respect to K and λ, C can be taken as a constant. The term $L(\lambda, K)$ in Eq. (30) can be regarded as the expectation of $\ln x_K(F)$, thus a natural estimate $\hat{L}(\lambda, K)$ of $L(\lambda, K)$ can be obtained from the probability of non-exceedance F_i, corresponding to the sample element $x_i (i = 1,2, \cdots, n)$

$$\hat{L}(\lambda, K) = \frac{1}{n} \sum_{i=1}^{n} [x_i \ln x_K(F_i|\lambda, K)], \tag{34}$$

$$\widehat{\mathrm{KL}}(\lambda, K) = C - \hat{L}(\lambda, K), \tag{35}$$

where $x_K(F_i)$ is written as $x_K(F_i|\lambda, K)$ to emphasize that the model features parameters λ and K. $\widehat{\mathrm{KL}}(\lambda, K)$ is a sample estimate of the KL entropy. Eq. (33) is then recast as

$$\min_{\lambda, K} \{\widehat{\mathrm{KL}}(\lambda, K)\} = C + \min_{\lambda, K} \{-\hat{L}(\lambda, K)\} = C + \min_{\lambda, K} \left\{-\frac{1}{n} \sum_{i=1}^{n} [x_i \ln x_K(F_i|\lambda, K)]\right\}. \tag{36}$$

If K is given, the minimization of $\widehat{\mathrm{KL}}(\lambda, K)$ will result in the best choice of λ, which is equivalent to the system of nonlinear equations in Eq. (17) and the transformation in Eqs. (20) and (21) [31]. The term $\hat{L}(\lambda, K)$ is the log-likelihood function. Hence the parameters (λ and K) which minimize the KL entropy estimate $\widehat{\mathrm{KL}}(\lambda, K)$ are maximum likelihood estimates. It should be noted that for a finite sample size n, the maximum likelihood estimates are often biased estimates of the true parameters. Akaike [32] proposed an unbiased estimate of $\hat{L}(\lambda, K)$, which was later named as Akaike information criterion (AIC) [33]. One of the AIC unbiased estimates of $-\hat{L}(\lambda, K)$ is given by

$$\hat{\Gamma}(\lambda, K) = -\hat{L}(\lambda, K) + \frac{K}{n}, \tag{37}$$

where $\hat{\Gamma}(\lambda, K)$, called differential entropy, are the unbiased estimates of $-\hat{L}(\lambda, K)$. By substituting Eq. (19) into the term $\ln x_K(F_i|\lambda, K)$ of Eq. (34) and considering Eq. (16), Eq. (37) can be expanded as

$$\hat{\Gamma}(\lambda, K) = \sum_{s=0}^{K} \lambda_s \left\{\frac{1}{n} \sum_{i=1}^{n} [x_i(F_i)^s]\right\} + \frac{K}{N} = \sum_{s=0}^{K} (\lambda_s b_s) + \frac{K}{N} = \hat{H}[x(F)] + \frac{K}{N}, \tag{38}$$

where b_s is the sample estimate of the type 2 PWM β_s in Eq. (4).

Given a sample of data and a specific order of K, the maximum entropy QF (with parameters λ) can be obtained by using the algorithm in Section 3.1. By increasing a model of sufficiently high order K, one can make the quantity $\mathrm{KL}[x(F), x_K(F)]$ in Eq. (30) as small as that one wants. This is because the more PWMs are used, the more information the MEP can extract from the sample of data. It is theoretically possible to approximate any QF $x(F)$ using $x_K(F)$ with an arbitrary degree of accuracy which depends on the order K. In other words, the function $-\hat{L}(\lambda, K)$ decreases as a function of K, approaching zero asymptotically.

For a constant of n, the term $\frac{K}{n}$ in Eq. (38) increases as a function of K. Consequently, the differential entropy $\hat{\Gamma}(\lambda, K)$ must have a minimum for a certain K value. That is to say; for a series of K, there does exist a number K to minimize the differential entropy $\hat{\Gamma}(\lambda, K)$ in Eq. (38), which in turn minimizes the term $\widehat{\mathrm{KL}}(\lambda, K)$ in Eq. (36). This K is the optimal order of the maximum entropy QF.

The term $\frac{K}{n}$ in AIC can be interpreted as a penalty term that prevents us from establishing too elaborate models which cannot be justified by the given sample of data. When only a sample of data is available, the MEP and the AIC are combined to determine the optimal order of PWMs being used in the estimation of a QF, thus preventing us from using either too sophisticated models (models with too many alterable parameters to properly contain the sample information) or too simple models (models with too little adjustable parameters to fully accommodate the sample information).

The existing optimal order in model selection acknowledged the fact that the information contained in a sample of data shouldn't produce a too complicated model, which may have redundant parameters, and shouldn't generate a too simple model in which too little information is used. AIC has been successfully used in the determination of maximum entropy distribution constrained by ordinary moments [34] and fractional moments [18, 35]. The present paper is to determine the optimal order of PWMs in MEP.

4. Case Studies

Two case studies from civil engineering are given; one is soil undrained shear strength in the Nipigon River landslide area, and the other is flood frequency analysis for the Grand River in Ontario, Canada.

4.1 Soil undrained shear strength

On April 23, 1990, a large landslide occurred on the east bank of the Nipigon River in the District of Thunder Bay in Northwestern Ontario, Canada (Fig. 1, adapted from [36]). The landslide involved approximately 300,000m^3 of soil and extended almost 350m inshore with a maximum width of approximately 290m. Soil from the landslide was pushed into the Nipigon River 300m upstream and downstream and formed several islands in the river. These islands redirected the river current and caused subsequent erosion on the west bank of the Nipigon River opposite the slide area. This likely caused several landslides to occur further south one month after the landslide. Since then, people have started to pay attention to the landslides of various scales frequently occurring in this area due to adverse landscape geology and soil properties of the upper silty sand layer.

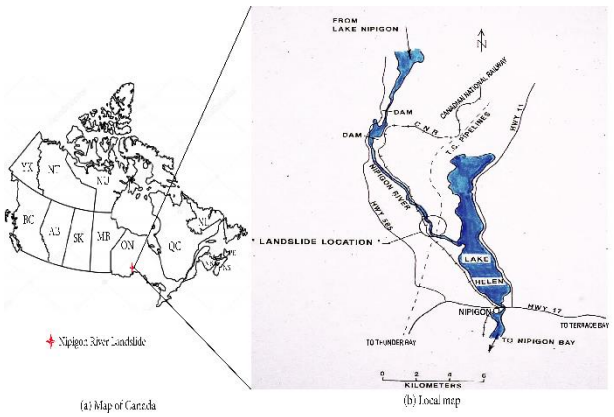

Figure 1. Location of Nipigon River landslide.

In order to investigate the mechanism of the landslides, soil properties are needed in undrained conditions because short-term slope stability requires the undrained shear strength of the soil. In the case of field investigation, the vane shear test (VST) is the most frequently adopted method to obtain the undrained shear strength of soil [37]. A complete outline of the vane shear test is provided by Walker [38]. The field test procedure followed the standards of ASTM D2573-08 [39]. The VST testing was carried out by graduate students (NS Kanwar, S Singh, and D Joshi) under the supervision of Dr. J Deng from Lakehead University, and the measured undrained shear strengths are listed in Table 1. Even if great care was taken and the strict standard was followed to keep the conditions of testing as homogeneous as possible, the values exhibit an intrinsic variability that cannot be ignored in slope stability analysis. The soil undrained shear strength is actually a random variable, and a probabilistic approach to treatment is appropriate. Maximum entropy QFs are used to characterize this soil's undrained shear strength.

Based on the sample in Table 1, ten-order sample PWMs can be calculated by using Eq. (5), the results of which are listed in Table 2. The third column is the normalized PWM by the sample mean (51.68471074 kPa). Eight digits to the right of the decimal point are kept to increase the calculation accuracy. The maximum entropy QFs can be obtained from the algorithm in Section 3.1 for the PWM order K from 1 to 10, of which the parameters are listed in Table 3. The differential entropy $\hat{\Gamma}(\lambda, K)$ in Table 3 indicates that the minimum value occurs at $K = 5$, so in accordance with the AIC in Section 3.3, the maximum entropy QF with $K = 5$ is the unbiased and optimal model from the soil sample in Table 1, the analytical function of which is given by

$$x_K(F) = \exp(2.737607 + 7.917811F - 33.2429746F^2 + 77.56007F^3 - 83.5084853F^4 + 33.31704F^5). \quad (39)$$

Table 1. Measured undrained shear strength (kPa) (n =121)

60.80	56.05	52.25	41.80	80.75	38.95	18.05	23.75
32.30	61.75	56.05	52.25	42.75	81.70	39.90	18.05
25.65	33.25	61.70	57.00	52.25	44.65	84.55	39.90
19.00	26.60	33.25	62.70	57.00	52.25	44.65	85.50
39.90	19.00	26.60	33.25	63.65	57.00	53.20	45.60
87.40	39.90	19.00	27.55	33.25	64.60	57.00	53.20
46.55	95.00	39.90	20.90	28.50	33.25	64.60	57.95
54.15	47.50	95.00	39.90	20.90	29.45	33.25	64.60
57.95	54.15	49.40	95.00	40.85	22.80	29.45	33.25
64.60	57.95	55.10	49.40	96.90	40.85	22.80	30.40
34.20	65.55	58.90	55.10	51.30	104.5	41.80	23.75
32.30	35.15	68.40	68.40	68.40	71.25	71.25	74.10
77.90	77.90	80.75	65.55	66.50	66.50	66.50	66.50
67.45	67.45	68.40	68.40	68.40	35.15	36.10	37.05
37.05	38.00	38.00	38.00	38.00	38.00	38.00	104.50
114.00							

Table 2. Sample PWMs for soil undrained shear strength

PWM Order	PWM	Normalized PWM
K=1	51.68471074	1.0
K=2	31.78724862	0.61502228
K=3	23.39131381	0.45257705
K=4	18.65441261	0.36092709
K=5	15.58642715	0.30156746
K=6	13.42819194	0.25980975
K=7	11.82289047	0.22875025
K=8	10.57950802	0.20469318
K=9	9.58623690	0.18547529
K=10	8.77319651	0.16974452

The corresponding QF curve for $K = 5$ is shown in Fig. 2, superposed by QFs with $K = 1$, $K = 10$, and the empirical quantiles of the sample based on the Gringorten plotting position formula [40]. Inspection of the curves in Fig. 2 shows that the difference between the optimal five-order model and the 10-order model is very small, so there seems to be no justification for the complication of adopting a 10-order model with 11 coefficients. It is also evident that the QF with $K = 1$ does not fit the sample as well as the optimal model. Therefore, it is reasonable to choose the model with $K = 5$ as the optimal QF. One can

draw the same conclusion from Fig. 3, where the quantile value is expressed as a semi-log plot of the probability of exceedance (POE). The probability of exceedance is cut at the quantile of 10^{-3} [22]. The model with $K = 1$ evidently underestimates the distribution tail region. This is because accurate modeling and extrapolation of the tail are not rational if only limited information is involved.

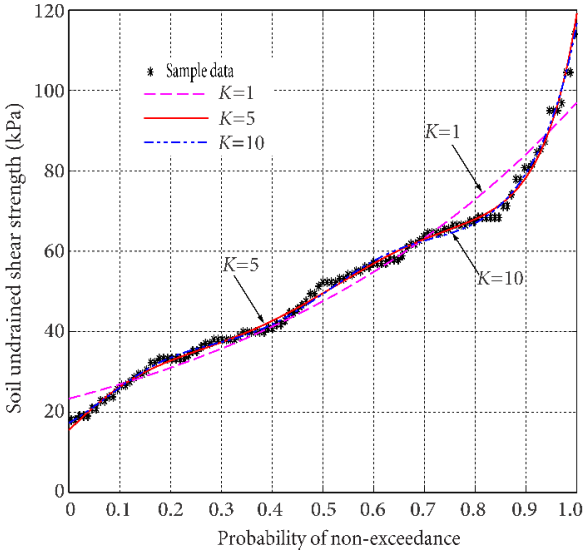

Figure 2. Maximum entropy quantile functions of soil undrained shear strength.

Table 3. Parameters of maximum entropy quantile functions (moment order K=1−10)

	K=1	K=2	K=3	K=4	K=5
λ_0	−3.1485742	4.79282214	−2.872965	−2.940865	−2.737607
λ_1	−1.4264077	−0.032497	−3.916489	−2.782127	−7.917811
λ_2		8.6442E−6	5.29956191	0.68083212	33.2429746
λ_3			−3.170614	3.54722833	−77.56007
λ_4				−3.197236	83.5084853
λ_5					−33.31704
$\hat{\Gamma}(\lambda, K)$	−4.162	−4.161	−4.235	−4.233	−4.261 (minimum)
	K=6	K=7	K=8	K=9	K=10
λ_0	−2.7239104	−2.807432	−2.855384	−2.753099	−3.945162
λ_1	−8.3984161	−4.398103	−2.575307	−7.463430	−4.16645
λ_2	37.5870965	−11.56287	−36.71253	32.2787573	−5.815689
λ_3	−93.761831	161.616299	326.477491	−110.4325	68.1260732
λ_4	112.324229	−554.8126	−1133.799	329.519011	30.3032168
λ_5	−57.635068	864.251273	2016.4031	−756.0733	−1063.242
λ_6	7.83238654	−635.6442	−1936.525	1043.36223	2986.67449
λ_7		178.616313	954.814281	−729.4156	−3719.649
λ_8			−189.9773	187.763121	2234.45903
λ_9				8.47675453	−528.4069
λ_{10}					−0.194222
$\hat{\Gamma}(\lambda, K)$	−4.253	−4.249	−4.243	−4.231	−4.242

A comparison of maximum entropy QFs for orders 1 to 5 is given in Fig. 4, which shows that with an increase in the PWM order, better QFs have been obtained. This observation is also consolidated in Fig. 5, where the quantile value is plotted versus a semi-log POE. The conclusion is somewhat obvious: the more PWM is employed, the more information is incorporated into MEP, which will then result in a better QF.

To further demonstrate the accuracy of the optimal maximum entropy QF, normal and lognormal distributions, the most commonly used probability functions in engineering [1], are assumed to fit the soil property by the method of moments. The PDFs of normal and lognormal distributions are given by, respectively,

$$f_1(x) = \frac{1}{\sigma\sqrt{2\pi}} \exp\left[-\frac{1}{2}\left(\frac{x-\mu}{\sigma}\right)^2\right] = \frac{1}{21.1043\sqrt{2\pi}} \exp\left[-\frac{1}{2}\left(\frac{x-51.6847}{21.1043}\right)^2\right], \tag{40}$$

$$f_2(x) = \frac{1}{\zeta\, x\sqrt{2\pi}} \exp\left[-\frac{1}{2}\left(\frac{\ln x-\kappa}{\zeta}\right)^2\right] = \frac{1}{0.4298\, x\sqrt{2\pi}} \exp\left[-\frac{1}{2}\left(\frac{\ln x-3.8582}{0.4298}\right)^2\right], \tag{41}$$

where X is the undrained shear strength, taking as a random variable.

Fig. 6 compares the maximum entropy, normal and lognormal QFs, accompanied by a semi-log plot of POE in Fig. 7. The normal distribution somewhat underestimates the sample tail region, while the lognormal distribution overestimates the sample tail region. The normal distribution is unacceptable for soil undrained shear strength due to its negative values of support. By contrast, the optimal maximum entropy QF lies between lognormal and normal QFs, which appears a better fit for the soil sample data.

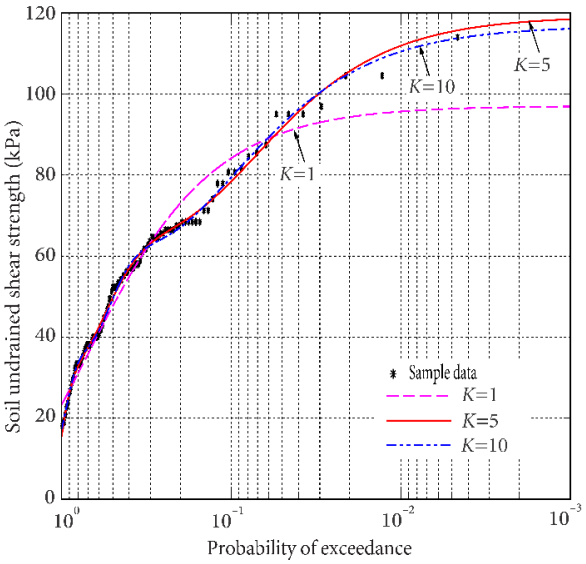

Figure 3. Semi-log plot of maximum entropy QF approximation of the sample tail region.

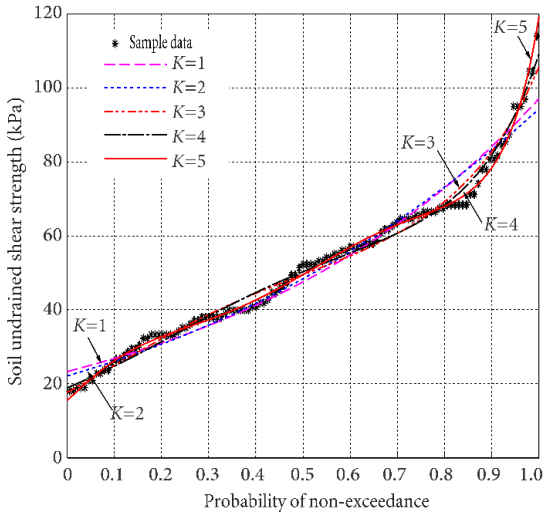

Figure 4. Comparison of maximum entropy quantile functions of soil undrained shear strength.

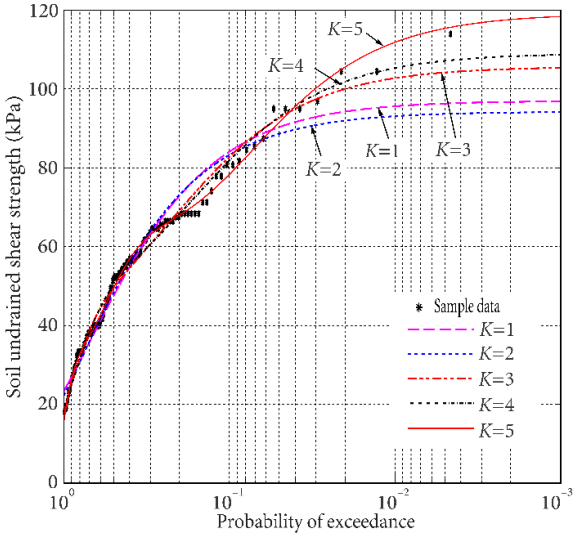

Figure 5. Semi-log plot of maximum entropy QF approximation of the sample tail region.

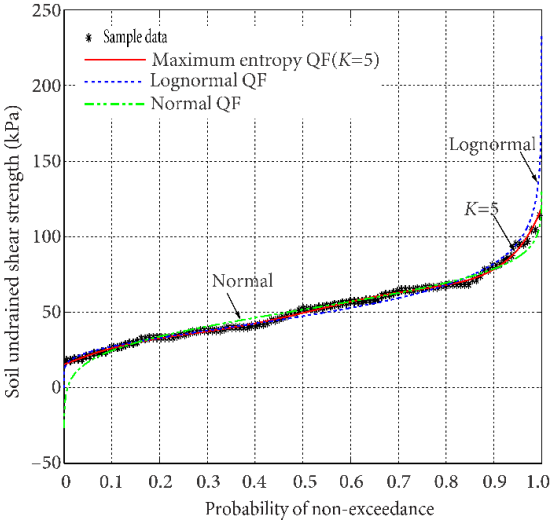

Figure 6. Comparison of three quantile functions.

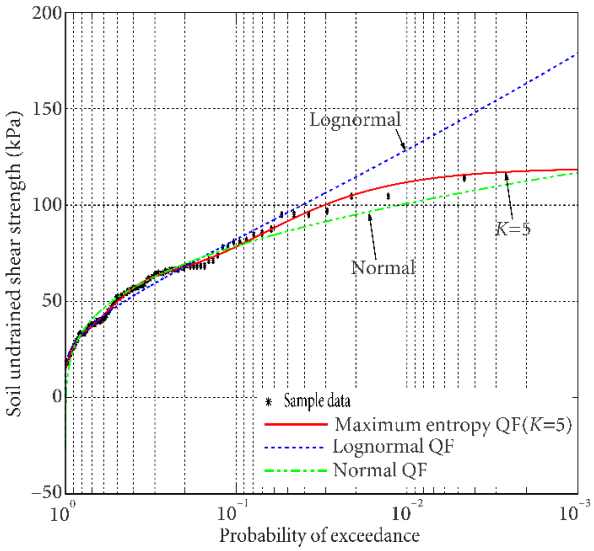

Figure 7. Semi-log plot of three quantile functions.

4.2 Flood frequency analysis

Three common data sets are usually used in flood frequency analysis: (1) peaks over a threshold (POT) model, (2) annual maximum series model, and (3) time series model. The time series flood model is described best by a stochastic process in continuous time. The POT model is devalued by the involvement of dependent observations. The annual maximum model is statistically more efficient than the POT model when ς is small ($\varsigma < 1.65$), where ς is the mean number of peaks per year included in the POT series [40]. The historical annual maximum daily discharge data of the Grand River in Ontario, Canada, is taken as an example [41], which is listed in Table 4. The Grand River watershed spans a length of 290km and covers an area of 6965 km^2. It is the largest of the watersheds in Southwestern Ontario that drain into Lake Erie, which is shown in Fig. 8 (adapted from Fig. 2 [42]).

Table 4. Annual maximum daily discharge of the Grand River, Ontario, Canada (m3/s)

331	841	379	490	855	253	323	476
680	561.5	558	351	530	173	501	719
653.5	1040	311	445	493	439	1070	351.5
428	685	430	657	127	697	459	527
759.5	470	425	402	374	524	179	367
538	343	382	657.5	478	498	561	357
264	248	456	654	1140	487	244	473
600	292	228	636	411	388	654.5	345
564	583	575	396	733	759	725	112
433							

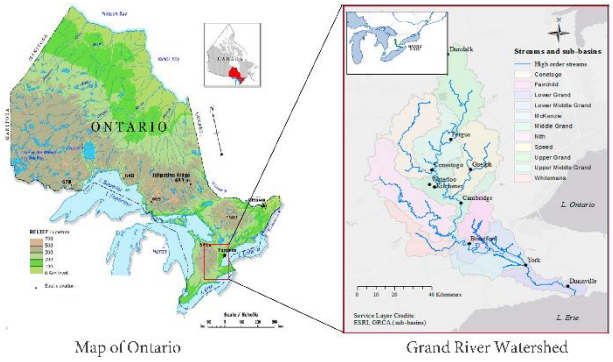

Figure 8. The Grand River, Southwestern Ontario, Canada.

Theoretically, the algorithm in Section 3.1, being used in Section 4.1, is equivalent to the one in Section 3.2, which is used in this section. Based on the sample in Table 4, ten-order sample PWMs can be calculated by using Eq. (5). From these sample PWMs, the maximum entropy QFs can be obtained by solving Eq. (28). The corresponding differential entropy of Eq. (38) versus PWM order is plotted in Fig. 9, which shows the optimal order of quantile function is $K = 7$. So the optimal quantile function is

$$x(F) = \exp(4.41357 + 22.92339F - 166.00783F^2 + 676.15183F^3 - 1566.7939F^4 + 2053.42095F^5 - 1412.42386F^6 + 395.52942F^7). \quad (42)$$

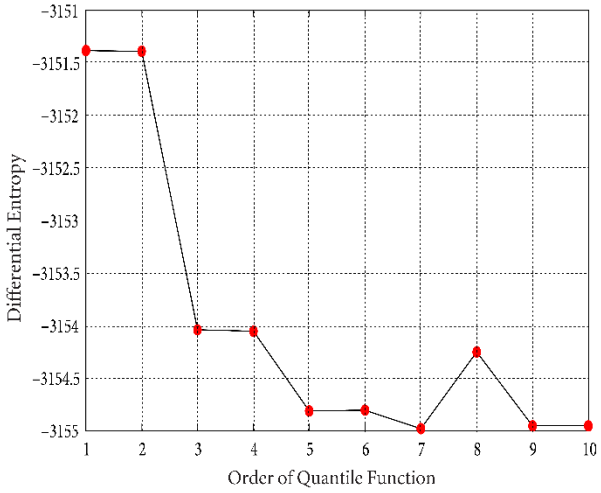

Figure 9. Differential entropy versus order of quantile function.

Fig. 10 shows that the maximum entropy QF with $K = 7$ is quite similar to that with $K = 5$, the functional form of which is

$$x(F) = \exp(4.59889 + 14.48539F - 62.47622F^2 + 133.28411F^3 - 132.63654F^4 + 49.87552F^5). \quad (43)$$

In order to demonstrate the advantage of the optimal maximum entropy quantile function, the comparison is made with normal, lognormal, Gumbel, and Gamma functions. The Gumbel distribution also called the extreme value type I distribution, is the distribution of the maximum (or the minimum) of a number of samples of various distributions [1,43] with $-\infty < x < +\infty$,

$$f(x,\mu,\sigma) = \frac{1}{\sigma}\exp\left(\frac{x-\mu}{\sigma}\right)\exp\left[-\exp\left(\frac{x-\mu}{\sigma}\right)\right]. \quad (44)$$

The Gamma distribution covers exponential, Erlang, and chi-square distributions as special cases

$$f(x,a,b) = \frac{1}{b^a\Gamma(a)}x^{a-1}\exp(-\frac{x}{b}), \quad 0 \le x < +\infty, \quad (45)$$

where $\Gamma(a)$ is the Gamma function.

These distribution function parameters are estimated by the method of maximum likelihood, which is listed in Table 5. Comparison of quantile functions for the annual maximum daily discharge is illustrated in Fig. 11. It appears that all QFs fit well the sample data points. Our attention is focused on the distribution tail in Fig. 12, where a semi-log plot is presented. Inspection of Fig.12 indicates that in the tail region, normal distribution underestimates the sample data points, but lognormal distribution overestimates the sample value. Gumbel and Gamma quantile functions generally fit better than normal and lognormal functions. The optimal maximum entropy QF lies between Gumbel and Gamma quantile functions.

This is rational because the optimal maximum entropy QF contains seven PWMs which are sure to attest more information than two ordinary moments in normal, lognormal, Gumbel, and Gamma functions. Another reason may come from the property of PWM that PWMs are only linear combinations of the observed sample values for any order PWMs, such that less bias and more efficiency can be achieved in moment estimate, as shown by Pandey [11]. The third advantage of the proposed model is that maximum entropy QFs are not confined to classical probability distributions, such as normal, lognormal, Gumbel, and Gamma functions. The choice of a maximum entropy QF depends on the sample information only; thus is objective, not subjective.

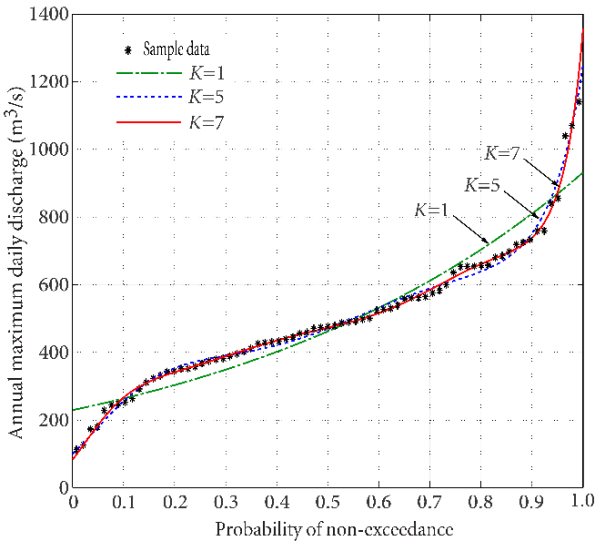

Figure 10. Maximum entropy quantile functions for annual maximum daily discharge.

Table 5. The parameters of Gumbel, lognormal, and gamma distributions

Distribution	parameters	Maximum likelihood estimate
Normal	μ	500.6849315
	σ	205.8026041
Lognormal	κ	6.126279
	ζ	0.447489
Gumbel	μ	-405.410729
	σ	172.927108
Gamma	a	5.735789
	b	87.291384

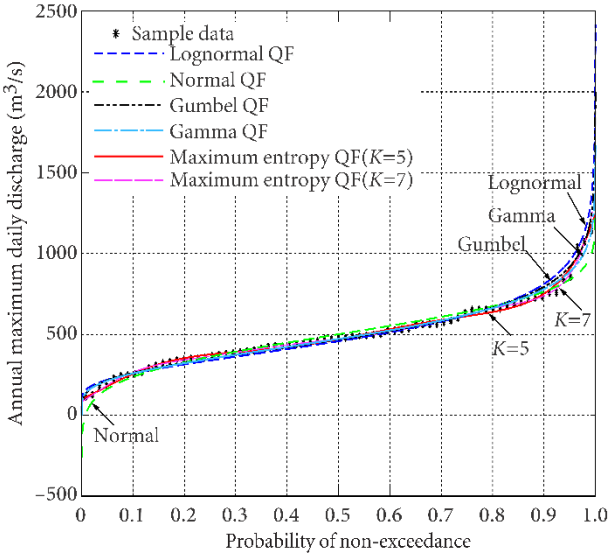

Figure 11. Comparison of quantile functions for annual maximum daily discharge.

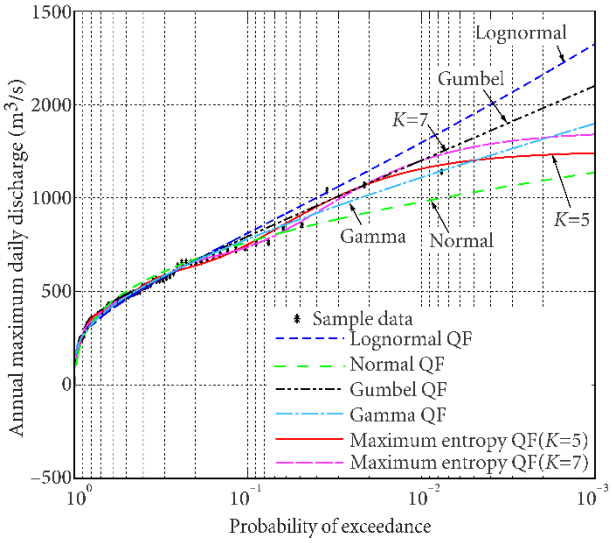

Figure 12. Semi-log plot for the sample tail region of maximum entropy and other quantile functions.

The fourth advantage of maximum entropy QFs is the capability to adjustment of model sophistication in accordance with the available sample information. The maximum entropy principle, together with the AIC, can avoid a too-simple model (e.g., the model $K = 1$ in Fig.10) and a too-elaborate model. Too simple models cannot extract enough information from the sample, and too elaborate models include too trivial and redundant information from an individual sample. Thus, both models cannot properly reflect the characteristics of the population from which the sample comes.

5. Reliability Analysis Based on Quantile Functions

5.1 Procedure of QF-based first-order reliability method

The basic concept of the QF-based first-order reliability method is to transform nonnormal random variables into equivalent normal random variables by using QFs, and then use the Hasofer-Lind method [1,43] to conduct the reliability analysis. The maximum entropy QF-based first-order reliability method was proposed recently [27]. The procedure is summarized as follows.

Step 1. Set up a limit state equation

$$Z = g_X(\boldsymbol{X}) = g_X(X_1, X_2, \cdots, X_n) = 0, \tag{46}$$

Determine the quantile distributions of basic random variables $X_i (i = 1, 2, \cdots, N)$, and calculate the correlation matrix $\rho_{\boldsymbol{X}}$.

Step 2. Assume the initial design values $\boldsymbol{x}^* = x_i^* (i = 1,2, \cdots, N)$, usually the mean values, and the initial reliability index β, usually $\beta = 3.0$. The probability of failure is $p_f = \Phi(-\beta)$, where Φ is the CDF of standard normal variables.

Step 3. For the non-normal random variable X_i, use the equivalent mean value $(\mu_{X_i'})$ and the equivalent standard deviation $(\sigma_{X_i'})$ to replace μ_{X_i} and σ_{X_i}, respectively,

$$\mu_{X_i'} = \mu_{X_i}, \tag{47}$$

$$\sigma_{X_i'} = \frac{\beta_i \sigma_{X_i}}{\beta}, \tag{48}$$

where for $\frac{\partial g_{\boldsymbol{X}}(\boldsymbol{X})}{\partial X_i} > 0$,

$$\beta_i = \frac{\mu_{X_i} - F_{X_i}^{-1}(p_f)}{\sigma_{X_i}} = \frac{\mu_{X_i} - \exp\left\{-\sum_{s=0}^{M}\left[\lambda_s (p_f)^s\right]\right\}}{\sigma_{X_i}}; \tag{49}$$

and for $\frac{\partial g_{\boldsymbol{X}}(\boldsymbol{X})}{\partial X_i} < 0$,

$$\beta_i = -\frac{\mu_{X_i} - F_{X_i}^{-1}(1-p_f)}{\sigma_{X_i}} = -\frac{\mu_{X_i} - \exp\left\{-\sum_{s=0}^{M}\left[\lambda_s (1-p_f)^s\right]\right\}}{\sigma_{X_i}}. \tag{50}$$

Step 4. Calculate the direction of cosines α_{X_i} at the values of the design point

$$\alpha_{X_i} = -\frac{\sum_{j=1}^{N}\left(\rho_{X_i X_j} \frac{\partial g_{\boldsymbol{X}}(x^*)}{\partial X_i} \sigma_{X_j}\right)}{\sqrt{\sum_{i=1}^{N}\sum_{j=1}^{N}\left(\rho_{X_i X_j} \frac{\partial g_{\boldsymbol{X}}(x^*)}{\partial X_i} \frac{\partial g_{\boldsymbol{X}}(x^*)}{\partial X_j} \sigma_{X_i} \sigma_{X_j}\right)}}, i = 1,2, \cdots, N, \tag{51}$$

where $\rho_{X_i X_j}$ is the correlation coefficient of the X_i and X_j variables, and $\rho_{X_i X_i} = 1$.

Step 5. Calculate the system reliability index

$$\beta = \frac{g_X(x^*) + \sum_{i=1}^{N}\left[\frac{\partial g_{\boldsymbol{X}}(x^*)}{\partial X_i}(\mu_{X_i} - x_i^*)\right]}{\sqrt{\sum_{i=1}^{N}\sum_{j=1}^{N}\left(\rho_{X_i X_j} \frac{\partial g_{\boldsymbol{X}}(x^*)}{\partial X_i} \frac{\partial g_{\boldsymbol{X}}(x^*)}{\partial X_j} \sigma_{X_i} \sigma_{X_j}\right)}}. \tag{52}$$

Step 6. Calculate the new design point $\boldsymbol{x}^* = x_i^*(i = 1,2,\cdots,N)$

$$x_i^* = \mu_{X_i} + \beta\alpha_{X_i}\sigma_{X_i},\ i = 1,2,\cdots,N. \quad (53)$$

Step 7. Repeat Steps 2 through 6 until β converges to a given tolerance level.

For illustrative purposes, two examples are considered in the next two sections by a nonlinear limit state function with (1) uncorrelated and (2) correlated random variables, respectively.

5.2 Example 1: Reliability with uncorrelated random variables

A cantilever steel beam is loaded by a bending moment B at the free end. The resisting moment capacity of a section is taken as YZ, where Y is the yield stress, and Z is the section modulus of the section [43, 44]. At the limit state of collapse in flexure, the performance function may be written as

$$g(\boldsymbol{X}) = YZ - B. \quad (54)$$

Random variables (RV) Y, Z, and B are assumed uncorrelated. The mean values for Z and B are 50in.^{3} and 1000kip·in., respectively. The corresponding coefficients of variation are 0.05 and 0.2, respectively. Z and B obey lognormal distribution and type 1 extreme asymptotic value (Gumbel)) distribution, respectively. Y's distribution must be determined from a sample of 50 elements which is listed in Table 6, and the sample is generated by Monte Carlo simulation supposing Y obeys lognormal distribution with the mean and the coefficients of variation are 40ksi and 0.125, respectively. This distribution is called parent lognormal distribution.

Table 6. A sample of 50 yield stresses (ksi).

36.2236	44.9545	41.3409	44.4594	39.5704
39.5391	32.2627	45.4191	42.7412	31.1391
40.8562	36.8796	44.9882	41.4602	45.0690
41.8553	38.3404	36.6011	46.3770	44.1867
37.8907	41.8362	40.9821	44.5629	39.6969
38.5396	32.2385	35.2878	40.8939	39.3426
51.0655	42.0918	33.6679	36.4218	29.1235
29.9619	34.1277	44.5353	36.5982	42.6698
52.3907	40.0196	39.6914	46.0424	30.2088
41.3950	43.0497	39.4206	32.4737	29.7355

Traditionally, the method of moments is used for estimating the probability density function. The PDF is then integrated to obtain the CDF, which needs to be inverted to obtain the QF. By contrast, maximum entropy QFs are directly inferred from a sample in terms of PWMs and thus are distribution-free, which constitutes a direct advantage to conventional distributions.

For random variable Z with lognormal distribution, the relations between parameters κ and ζ to mean and standard deviation are

$$\zeta = \sqrt{\ln\left[1 + \left(\frac{\mu_X}{\sigma_X}\right)^2\right]} = 0.04996879,$$
$$\kappa = \ln\mu_X - \frac{1}{2}\zeta^2 = 3.91077456. \quad (55)$$

The lognormal distribution can be obtained as,

$$f(z) = \frac{1}{0.04996879\, z\sqrt{2\pi}}\exp\left[-\frac{1}{2}\left(\frac{\ln z - 3.91077456}{0.04996879}\right)^2\right], \quad (56)$$

where $f(z)$ is the lognormal PDF for Z.

For random variable B with Gumbel distribution, the relations between parameters α and u to mean and the standard deviation is

$$\alpha = \frac{\pi}{\sqrt{6}\sigma_B} = 0.00641275,$$
$$u = \mu_B - \frac{0.5772157}{\alpha} = 909.989358. \quad (57)$$

The Gumbel distribution can be obtained as,

$$F(b) = \exp\{-\exp[-0.00641275(b - 909.989358)]\}, \quad (58)$$

where $F(b)$ is the Gumbel CDF for the moment B.

Random variable Y's distribution is determined by conventional methods from the sample of 50 elements: firstly, assume normal or lognormal distribution, and then use the method of moments to calculate the parameters. The normal and lognormal distribution can be obtained as, respectively,

$$f_{Y1}(y) = \frac{1}{5.37394747\sqrt{2\pi}}\exp\left[-\frac{1}{2}\left(\frac{y - 39.60451139}{5.37394747}\right)^2\right], \quad (59)$$

$$f_{Y2}(y) = \frac{1}{0.13937469\, y\sqrt{2\pi}}\exp\left[-\frac{1}{2}\left(\frac{\ln y - 3.66961379}{0.13937469}\right)^2\right], \quad (60)$$

where $f_{Y1}(y)$ and $f_{Y2}(y)$, respectively, are the normal and lognormal PDFs for Y.

Based on the same sample data, the optimal maximum entropy QF is fitted by using the methodology in Section 3. The result is

$$y_K(F) = \exp(3.31148365 + 1.63566312F - 2.47119017F^2 + 1.45463938F^3). \quad (61)$$

A comparison of the optimal maximum entropy, normal, and lognormal QFs from the same sample of 50 elements is shown in Fig. 13, together with the sample data points. Fig. 14 compares various orders of maximum entropy QFs, and Fig. 15 illustrates the semi-log plot for the sample tail region of maximum entropy QFs, normal QF, and lognormal QF. Figs. 13-15 shows that the optimal maximum entropy QF fits the sample data very well.

Three reliability analyses are conducted by assuming that random variable Y obeys three different probability functions: the normal distribution in Eq. (59), the lognormal distribution in Eq. (60), and the optimal entropy QF in Eq. (61). The results are listed in the upper half of Table 7. By comparison, the reliability analysis is also listed for the case that the lognormal parent distribution is used for Y with the mean and the coefficients of variation are 40ksi and 0.125, respectively. This case may be regarded as the exact result. The closer the reliability index is to the parent case, the better the distribution that Y is modeled. It is found that the optimal entropy QF results in a very accurate and efficient result, with the reliability index very close to the case of the parent distribution and with the smallest number of total iterations. In this example, the normal distribution gives the most conservative reliability index as compared to the lognormal and the maximum entropy QFs, although these QFs are modeled from the same sample.

The order of maximum entropy (ME) QF plays a significant role in the results of reliability analysis, as shown in the lower half of Table 7. Among this maximum entropy QFs, the optimal QF yields the most conservative reliability index, and the calculation is the most efficient. The detailed iteration calculations are tabulated in Table 8 for the case of the optimal maximum entropy QF.

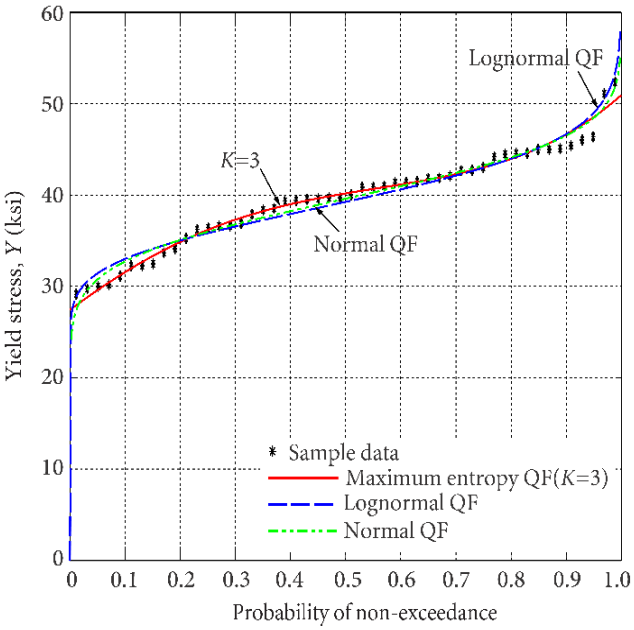

Figure 13. Sample-based three quantile functions.

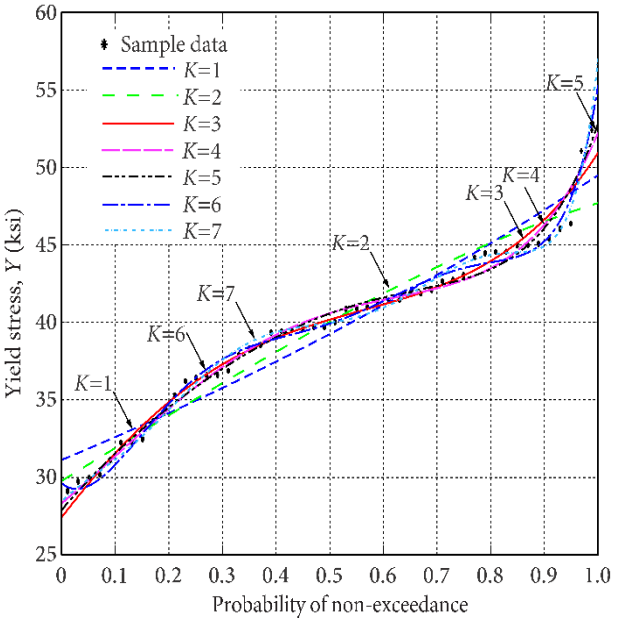

Figure 14. Sample-based maximum entropy QFs.

Table 7. Results of reliability analysis with different QF of Y for example 1

Sample-based QF of Y	β	p_f	Total Iter. No.	Final design point $\{Y, Z, B\}$
ME QF (K=3)	2.6072	0.00456	7	{32.4087,48.7327, 1579.3638}
Lognormal QF	2.5856	0.00486	12	{32.0799,48.7646, 1564.3641}
Normal QF	2.4841	0.00649	12	{30.6237,48.9046, 1497.6395}
Parent Lognormal QF	2.6869	0.00361	12	{33.4006,48.6468, 624.8299}
ME QF (K=1)	2.8230	0.00238	12	{36.0693,48.3717,1744.7336}
ME QF (K=2)	2.7559	0.00293	10	{34.8537,48.4929,1690.1569}
ME QF (K=4)	2.6677	0.00382	9	{33.3639,48.6396, 1622.8061}
ME QF (K=5)	2.6408	0.00416	8	{32.9327,48.6817,1603.2223}
ME QF (K=6)	2.739	0.00308	9	{34.5631,48.5216,1677.0570}
ME QF (K=7)	2.6762	0.00372	9	{33.5021,48.6261,1629.0759}

5.3 Example 2: Reliability with correlated random variables

Consider the same problem in Section 5.2, except assuming that the design variables Y and Z are now partially correlated with a correlation coefficient $\rho_{YZ} = 0.4$. The correlation matrix is

$$C = \begin{bmatrix} 1.0 & 0.4 & 0 \\ 0.4 & 1.0 & 0 \\ 0 & 0 & 1.0 \end{bmatrix} \quad (62)$$

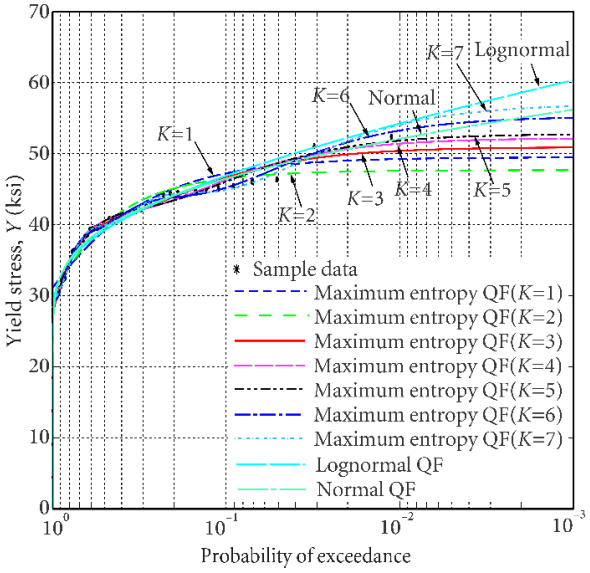

Figure 15. Semi-log plot for the sample tail region of maximum entropy, normal, and lognormal QF.

Three reliability analyses are conducted by assuming that random variable Y obeys three different probability functions: the normal distribution in Eq. (59), the lognormal distribution in Eq. (60), and the optimal maximum entropy QF in Eq. (61). The results are listed in the upper half of Table 9. By comparison, the reliability analysis is also listed for the case that the parent lognormal distribution is used for Y with the mean and the coefficients of variation are 40ksi and 0.125, respectively. This case may be regarded as the exact result. It is observed in Table 9 that the optimal maximum entropy QF results in comparable results to the case of lognormal QF but better results than the case of normal QF. The use of the optimal maximum entropy QF also leads to an efficient algorithm, with the smallest number of only 7 total iterations.

The lower half of Table 9 shows the significant effect of orders of maximum entropy QFs on the results of reliability analysis with correlated random variables. Among these maximum entropy QFs, the optimal QF yields the most conservative reliability index, and the calculation is the most efficient, which suggests that the optimal QF generates results more similar to the conventional QFs, such as normal and lognormal QFs than any other maximum entropy QFs. The detailed iteration calculations are tabulated in Table 10 for the case of the optimal maximum entropy QF.

To investigate the effect of the correlation coefficient of random variables on the reliability analysis of structures, the variation of the correlation coefficient ρ_{YZ} versus the reliability index is shown in Table 11. Positive values of the correlation coefficient would lead to smaller reliability indexes. Results from sample-based optimal maximum entropy QF are close to those with the parent QF, especially when the correlation coefficient is negative. Table 11 shows that the sample-based normal QF always leads to the smallest reliability index, regardless of positive or negative correlation coefficients. Therefore, the use of normal QFs would result in conservative reliability results in this example.

Table 8. Iterative calculations for Example 1 using the optimal maximum entropy QF (K=3)

Iter No.		Assumed design point $\boldsymbol{x}^*$	p_f	$\sigma'^{N}_{X_i}$	β_i	New β	New $\boldsymbol{x}^*$
1	Y	39.6045	$\beta_0 = 3$	4.0394	2.2550	2.5514	$39.6045 - 2.123\beta$
	Z	50	0.00135,	2.3381	2.8057		$50 - 0.56353\beta$
	B	1000		313.4295	4.7014		$1000 + 255.6994\beta$
2	Y	34.1866	0.00536	4.6794	2.2216	2.6093	$39.6045 - 2.853\beta$
	Z	48.5622		2.3672	2.4159		$50 - 0.5141\beta$
	B	1652.387		284.0831	3.6240		$1000 + 216.5472\beta$
3	Y	32.1595	0.00454	4.5897	2.2285	2.6071	$39.6045 - 2.754\beta$
	Z	48.6587		2.3634	2.4667		$50 - 0.4827\beta$
	B	1565.035		287.8259	3.7551		$1000 + 222.6079\beta$
4	Y	32.4238	0.00457	4.5930	2.2283	2.6072	$39.6045 - 2.760\beta$
	Z	48.7416		2.3635	2.4648		$50 - 0.4863\beta$
	B	1580.364		287.6847	3.7501		$1000 + 222.1829\beta$
5	Y	32.4074	0.00456	4.5928	2.2283	2.6072	$39.6045 - 2.759\beta$
	Z	48.7322		2.3635	2.4649		$50 - 0.4861\beta$
	B	1579.284		287.6929	3.7504		$1000 + 222.2154\beta$
6	Y	32.4088	−0.0046	4.5929	2.2283	2.6072	$39.6045 - 2.759\beta$
	Z	48.7327		2.3635	2.4649		$50 - 0.4861\beta$
	B	1579.368		287.6927	3.7504		$1000 + 222.2138\beta$
7	Y	32.4087	−0.0046	4.5929	2.2283	2.6072	$39.6045 - 2.759\beta$
	Z	48.7327		2.3635	2.4649		$50 - 0.4861\beta$
	B	1579.364		287.6927	3.7504		$1000 + 222.2138\beta$

Table 9. Results of reliability analysis with different QF of Y for example 2

Sample-based QF of Y	β	p_f	Total Iter No.	Final design point (Y, Z, B)
ME QF(K=3)	2.4861	0.00646	7	{31.6899,47.4664,1504.2026}
Lognormal QF	2.4882	0.00642	11	{31.7192,47.4653,1505.5619}
Normal QF	2.3919	0.00837	11	{30.4740,47.5189,1448.0930}
Parent Lognormal QF	2.5917	0.00478	11	{32.9555,47.4069,1562.3177}
ME QF(K=1)	2.7346	0.00312	11	{35.3370,47.4253,1675.8685}
ME QF(K=2)	2.6539	0.00398	9	{34.0851,47.4171,1616.2166}
ME QF(K=4)	2.5520	0.00535	8	{32.5973,47.4389,1546.3810}
ME QF(K=5)	2.5229	0.00582	8	{32.1919,47.4499,1527.5031}
ME QF(K=6)	2.6305	0.00426	8	{33.7345,47.4194,1599.6693}
ME QF(K=7)	2.5623	0.00520	8	{32.7429,47.4354,1553.1727}

6. Conclusions

In this paper, the maximum entropy principle (MEP) is integrated with another information principle, the Akaike information criterion (AIC), to directly derive an analytical quantile function (QF) from an observed sample of data. The MEP is constrained by integral probability-weighted moments (PWMs) and is used to estimate a series of QFs, where PWMs are interpreted as the moments of QF. The MEP with normalization is constructed in a conventional probabilistic sense, and normalization is mainly designed to remove the effect of dimension in sample data and to prevent overflow and underflow in the calculation. A more general formulation is developed for the PWM-based MEP, where the normalization condition is relaxed. The AIC is then used to locate the optimal order of PWMs in such a way that the estimated QF can properly catch the information in a given sample of data.

An illustrative case study is given for modeling the maximum entropy QF from a sample of data. The maximum entropy QF with order $K = 5$ is found to be the optimal model for the soil sample of undrained shear strength from the Nipigon River landslide area. The sample was obtained by field vane shear testing. The optimal maximum entropy QF lies between lognormal and normal QFs, which appears to be the best fit for the soil sample data. The normal distribution underestimates the sample data in the tail region, but the lognormal distribution overestimates the tail value. Furthermore, the negative value of support in a normal distribution is a defect for the positive values of soil undrained shear strength. By contrast, the optimal maximum entropy QF lies between lognormal and normal QFs, which appears to be a better QF for the soil sample data.

Table 10. Iterative calculations for Example 2 using the optimal maximum entropy QF (K=3)

		$\boldsymbol{x}^*$	p_f	$\sigma_{X_i'}^N$	β_i	New β	New $\boldsymbol{x}^*$
1	Y	39.6045	$0.00135, \beta_0 = 3$	4.0394	2.2549	2.4311	$39.6045 - 2.3945\beta$
	Z	50		2.3381	2.8057		$50 - 1.005\beta$
	B	1000		313.4295	4.7014		$1000 + 243.6488\beta$
2	Y	33.7831	0.00753	4.8713	2.2037	2.4830	$39.6045 - 3.303\beta$
	Z	47.5556		2.3754	2.3099		$50 - 1.0558\beta$
	B	1592.3452		276.3543	3.3593		$1000 + 196.3099\beta$
3	Y	31.4038	0.00651	4.7876	2.2121	2.4859	$39.6045 - 3.1857\beta$
	Z	47.3785		2.3719	2.3558		$50 - 1.0161\beta$
	B	1487.4465		279.6834	3.4723		$1000 + 202.8246\beta$
4	Y	31.6852	0.00646	4.7831	2.2126	2.4860	$39.6045 - 3.1842\beta$
	Z	47.4741		2.3717	2.3583		$50 - 1.0191\beta$
	B	1504.2003		279.8663	3.4786		$1000 + 202.7866\beta$
5	Y	31.6885	0.00646	4.7828	2.2126	2.4861	$39.6045 - 3.1836\beta$
	Z	47.4664		2.3716	2.3584		$50 - 1.0191\beta$
	B	1504.1374		279.8764	3.4789		$1000 + 202.8127\beta$
6	Y	31.6898	0.00646	4.7828	2.2126	2.4861	$39.6045 - 3.1836\beta$
	Z	47.4664		2.3716	2.3584		$50 - 1.0191\beta$
	B	1504.2034		279.8767	3.4789		$1000 + 202.8124\beta$

The proposed method is also applied in the flood frequency analysis of the Grand River in Ontario. In the tail region of the flood QFs, normal distribution underestimates the sample data, but lognormal distribution overestimates the sample value. Gumbel and Gamma quantile functions generally fit better than normal and lognormal functions. The optimal maximum entropy QF lies between Gumbel and Gamma quantile functions.

The optimal maximum entropy QF can be directly used in QF-based first-order reliability analysis. Examples with correlated and uncorrelated random variables are presented for illustration of the application of sample-based optimal maximum entropy QF to reliability analysis of structures. Reliability analysis results from sample-based optimal maximum entropy QF are generally better than those of normal and lognormal distributions from the same sample by obtaining closer to those with the parent QF, especially when the correlation coefficient is negative. In these two application examples, the use of optimal maximum entropy QFs also leads to an efficient algorithm with the smallest number of iterations in the calculation of the reliability index. Sample-based normal QFs yield the smallest reliability index, regardless of positive or negative correlation coefficients. The use of normal QFs would result in conservative reliability results. Among those maximum entropy QFs with various orders, the optimal QF yields the most conservative reliability index.

Table 11. Reliability index vs. correlation coefficient ρ_{YZ}

ρ_{YZ}	Sample-based optimal entropy QF	Sample-based normal QF	Sample-based lognormal QF	Parent lognormal QF
0.8	2.3725	2.3078	2.3989	2.5039
0.4	2.4861	2.3919	2.4882	2.5917
0.2	2.5457	2.4369	2.5359	2.6383
0	2.6072	2.4841	2.5856	2.6870
−0.2	2.6705	2.5334	2.6376	2.7377
−0.4	2.7355	2.5850	2.6920	2.7908
−0.8	2.8703	2.6959	2.8089	2.9045

Maximum entropy QFs are directly inferred from a sample of data in terms of PWMs and are free from classical probability distributions such as normal, lognormal, and Gumbel distributions, which constitute a prominent advantage to conventional distributions. Maximum entropy QFs have the capability of automatic adjustment of model sophistication based on the available sample information only, thus avoiding arbitrary and subjective choice of probability distributions. The maximum entropy QFs are applied to random variables that take only positive values. If the sample normalization condition is relaxed, the algorithm in Section 3.2 may be applied to censored or truncated samples. How to deal with censored or truncated sample data [45] in PWM-based MEP and in reliability analysis deserves future research.

7. Declaration of Competing Interest

The authors declare that the present study did not have any conflict of interest.

8. Acknowledgements

The author would like to acknowledge the financial support from the Natural Sciences and Engineering Research Council of Canada through discovery grants and in part by funding from the Government of Canada's New Frontiers in Research Fund (NFRF) [NFRFR-2021-00262].

9. References

[1] A. Haldar and S. Mahadevan. *Probability, Reliability and Statistical Methods in Engineering Design*. John Wiley, New York, 2000.

[2] M. Holicky. *Introduction to Probability and Statistics for Engineers*, Springer, 2013.

[3] E. Paloheimo and M. Hannus. "Structural design based on weighted fractiles." *Journal of the Structural Division - ASCE*, Vol. 100, No. ST7, pp. 1367-1378, 1974.

[4] F. Nishino, A. Hasegawa, C. Miki, and Y. Fujino. "A fractile-based reliability structural design." *Journal of Japan Society of Civil Engineers*, No. 326, pp. 141-153, 1982.

[5] M. Moustapha, B. Sudret, J. Bourinet, and B. Guillaume. "Quantile-based optimization under uncertainties using adaptive kriging surrogate models." *Structural and Multidisciplinary Optimization*, Vol. 54, No. 6, pp. 1403-1421, 2016.

[6] C. Zhang and A. Shafieezadeh. "A quantile-based sequential approach to reliability-based design optimization via error-controlled adaptive Kriging with independent constraint boundary sampling." *Structural and Multidisciplinary Optimization*. Vol. 63, pp. 2231–2252, 2021.

[7] G. Li, H. Yang, and G. Zhao. "A new efficient decoupled reliability-based design optimization method with quantiles." *Structural and Multidisciplinary Optimization*, Vol. 61, No. 2, pp. 635–647, 2020.

[8] W. He, H. Yang, G. Zhao, Y. Zeng, and G. Li. "A quantile-based sora method using maximum entropy method with fractional moments." *Journal of Mechanical Design*, Vol. 143, No. 4, pp. 041702.

[9] J. Ching, and K.K. Phoon. "A quantile-based approach for calibrating reliability-based partial factors." *Structural Safety*, Vol. 33, No. 4-5, pp. 275-285, 2011.

[10] W. Gilchrist. *Statistical Modelling with Quantile Functions*. Chapman & Hall/CRC, 2000.

[11] M.D. Pandey. "Direct estimation of quantile functions using the maximum entropy principle." *Structural Safety*, Vol. 22, No. 1, pp. 61–79, 2000.

[12] J. Deng and M.D. Pandey. "Using partial probability weighted moments and partial maximum entropy to estimate quantiles from censored samples." *Probabilistic Engineering Mechanics*, Vol. 24, No. 3, pp. 407-417, 2009.

[13] M. Holicky. *Reliability Analysis for Structural Design*. SUNN MeDIA, Stellenbosch, 2009.

[14] T. Sugiyama, Y. Fujino, and M. Ito. "A method to determine fractile values from statistical data." *Proc. of JSCE Structural Engineering /Earthquake Engineering*, Vol. 2, No. 2, pp. 45-55, 1985.

[15] R. Schöbi and B. Sudret. "PC-Kriging: a new meta-modelling method and its applications to quantile estimation." In: J. Li and Y. Zhao (eds). *Proceedings of the 17th IFIP WG7.5 conference on reliability and optimization of structural systems*, Taylor & Francis, New York, 2014.

[16] N. Razaaly, D. Crommelin, and P.M. Congedo. "Efficient estimation of extreme quantiles using adaptive kriging and importance sampling." *International Journal for Numerical Methods in Engineering*, Vol. 121, No. 9, pp. 2086-2105, 2020.

[17] W. Shen, M. Ohsaki, and M. Yamakawa. "Quantile-based sequential optimization and reliability assessment for shape and topology optimization of plane frames using L-moments." *Structural Safety*, Vol. 94, pp. 102153, 2022.

[18] X. Zhang, Y.M. Low, and C.G. Koh. "Maximum entropy distribution with fractional moments for reliability analysis." *Structural Safety*, Vol. 83, pp. 101904, 2020.

[19] A. Cicirello and R.S. Langley. "Probabilistic assessment of performance under uncertain information using a generalized maximum entropy principle." *Probabilistic Engineering Mechanics*, Vol. 53, pp. 143-153, 2018.

[20] J.A. Greenwood, J.M. Landwehr, N.C. Matalas, and J.R. Wallis. "Probability weighted moments: definition and relation to parameters of several distributions expressible in inverse form." *Water Resource Research*, Vol. 15, No. 5, pp. 1049-1054, 1979.

[21] J.R.M. Hosking and J.R. Wallis. *Regional Frequency Analysis: An Approach Based On L-Moments*. UK: Cambridge University Press, 1997.

[22] M.D. Pandey. "Extreme quantile estimation using order statistics with minimum cross-entropy principle." *Probabilistic Engineering Mechanics*, Vol. 16, No. 1, pp. 31-42, 2001.

[23] V.P. Singh. *Entropy Theory in Hydrologic Science and Engineering*. McGraw-Hill Education, 2015.

[24] V.P. Singh. *Entropy Theory in Hydraulic Engineering: An Introduction*. American Society of Civil Engineers, 2014.

[25] J. Deng and M.D. Pandey. "Derivation of sample-oriented quantile function using maximum entropy and self-determined probability weighted moments." *Environmetrics*, Vol. 21, No. 2, pp.113–132, 2010.

[26] J. Deng and M.D. Pandey. "Estimation of quantile function from censored samples using partial minimum cross entropy and partial probability." *Journal of Hydrology*, Vol. 363, No. 1–4, pp. 18–31, 2008.

[27] J. Deng and M.D. Pandey. "Optimal maximum entropy quantile function for fractional probability weighted moments and its applications in reliability analysis." *Applied Mathematical Modelling*, Vol. 114, pp. 230–251, 2023.

[28] T. Haktanir and A. Bozduman. "A study on sensitivity of the probability-weighted moments method on the choice of the plotting position formula." *Journal of Hydrology*, Vol. 168, No. 1–4, pp. 265-281, 1995.

[29] E.T. Jaynes. "On the rationale of maximum entropy methods." *Proceedings of IEEE*, Vol. 70, pp. 939-952, 1982.

[30] K.P. Burnham and D.R. Anderson. *Model Selection and Multimodel Inference: A Practical Information-Theoretic Approach* (2nd ed.), Springer-Verlag, 2002.

[31] J.N. Kapur and H.K. Kesavan. *Entropy Optimization Principles with Applications*. Academic Press, 1992.

[32] H. Akaike. "Information theory and an extension of the maximum likelihood principle," In: B.M. Petrov and F. Caski (Eds.), *Sec. Int. Symp. on Information Theory*, Akademiai Kiado, Budapest, pp. 267-281, 1973.

[33] Y. Sakamoto, M. Ishiguro, and G. Kitagawa. *Akaike Information Criterion Statistics*. Reidel, Dordrecht, 1986.

[34] D.R. Baker. "Probability estimation and information principles." *Structural Safety*, Vol. 9, pp. 97-116, 1990.

[35] P.L. Novi Inverardi and A. Tagliani. "Maximum entropy density estimation from fractional moments." *Communications in Statistics - Theory and Methods*, Vol. 32, pp. 2327-2345, 2003.

[36] R.B. Dodds, J.P. Burak, and K.D. Eigenbrod. "Nipigon River Landslide." In: *Proceedings of Third International Conference on Case Histories in Geotechnical Engineering*. MSO: St. Louis; Paper No 2.49, 1993.

[37] A. Jay, S. Nagaratnam, and D. Braja. *Correlations of Soil and Rock Properties in Geotechnical Engineering*. New Delhi: Springer. 2016.

[38] B.F. Walker. "Vane shear strength testing." In: M. Ervin (Ed.). *In Situ Testing for Geotechnical Investigations*. Rotterdam: A A Balkema. pp. 65-72, 1983.

[39] ASTM D2573-08. *Standard Test Method for Field Vane Shear Test in Cohesive Soil*. ASTM International (ASTM), 2008.

[40] A.R. Rao and K.H. Hamed. *Flood Frequency Analysis.* New York: CRC Press, 2000.

[41] N.C. Lind, H.P. Hong, and V. Solana. "A cross entropy method for flood frequency analysis." *Stochastic Hydrology and Hydraulics*, Vol. 3, pp. 191-202, 1989.

[42] A. Hanief and A.E. Laursen. "Modeling the natural drainage network of the grand river in southern Ontario: agriculture may increase total channel length of low-order streams*." Geosciences*, Vol. 9, pp. 46, 2019.

[43] G. Zhao. *Reliability Theory and Applications for Engineering Structures*. Dalian: Dalian University of Technology press, 1996.

[44] M. Zhang and F. Jin. *Structural Reliability Computations*. Beijing: Scientific Press, 2015.

[45] F. Yousefzadeh. "Nonparametric Estimation of the Family of Risk Measures Based on Progressive Type II Censored Data." *International Journal of Reliability, Risk and Safety: Theory and Application*, Vol. 5, No. 1, pp. 69-75, 2022.